ACTIVE MEDIA

PACS numbers: 42.70.Hj; 42.55.Rz; 42.25.Gy
DOI: 10.1070/QE2003v033n10ABEH002515

Interferometric study of electronic changes in the refractive index of a Nd : YAG laser crystal caused by intense pump

O.L. Antipov, O.N. Eremeikin, A.P. Savikin

***Abstract*. Changes in the refractive index of a Nd : YAG laser crystal caused by intense pump are measured using a polarisation interferometer. A significant electronic component in the refractive-index changes associated with the excitation of the $^4F_{3/2}$ electronic level of Nd^{3+} ions is revealed in the crystal pumped by 808-nm radiation of a pulsed diode array. An appreciable increase in the electronic component of the refractive index, which is caused by the population of the $^2F(2)_{5/2}$ high-energy level, is observed in a Nd : YAG crystal additionally pumped by a 266-nm laser beam. Analytic calculations show that the short-wavelength $4f - 5d$ transitions provide a predominant contribution to the polarisability of excited Nd^{3+} ions at the 1064.2-nm lasing transition.**

Keywords: *Nd : YAG laser crystal, intense laser pump, electronic levels of Nd^{3+} ions, polarisability, refractive-index changes.*

1. Introduction

Dynamic changes in the refractive index (RI) appearing in laser crystals and glasses upon intense pumping may be caused not only by their heating but also by changes in the population of the excited levels of activator ions [1 – 4]. The relation of RI changes to changes in the population of electronic levels of rare-earth ions is explained by different polarisabilities of these levels. The existence of the electronic component of RI changes in laser media has been long known [1, 2]. However, up to now, the issue of the value and dynamics of these RI changes remains little studied even for such widespread laser media as Nd : YAG crystals. Recent results of nonlinear-optics experiments indicate the necessity of further studying the mechanisms of RI changes in crystals doped with Nd^{3+} ions associated with the excitation of their various electronic states [5, 6]. The absence of precise data on the polarisability of Nd^{3+} electronic levels and on the influence of their population on the laser-crystal RI changes requires additional measurements.

The question of the mechanisms of RI changes seems to be especially important for laser media exposed to intense pumping. A significant progress in the field of solid-state lasers in the recent decade is associated with the use of high-power laser and diode-laser pump [7]. Recent studies have shown that narrow-band laser pumping reduces heat-induced RI changes but does not completely removes induced active-media distortions [8, 9]. In this case, taking into account the electronic component of the RI becomes essentially necessary.

This work is devoted to studying electronic changes in the RI of a Nd : YAG laser crystal caused by intense pump. Using a Jamin – Lebedev polarisation interferometer, we measured the RI changes in this crystal pumped by a 808-nm diode laser and also under combined pump by the same diode laser and the 266-nm fourth harmonic of an additional pulsed Nd : YAG laser. Different contributions to the polarisability of the excited level and to the electronic changes in the crystal's RI at the lasing-transition frequency are analytically estimated.

2. Theoretical description of electronic changes in the refractive index

Changes in the RI Δn_e of a medium upon changes in the populations of its energy levels can be described by the expression following from the Lorentz – Lorenz formula that relates the RI n of the medium to the polarisability p of the particles constituting it:

$$\Delta n_e(\nu) = \frac{2\pi F_L^2}{n_0} \sum_q \Delta N_q \Delta p_q(\nu), \quad (1)$$

where $F_L = (n_0^2 + 2)/3$ is the local-field (Lorentz) factor, n_0 is the refractive index, ΔN_q is the change in the population at the qth level, and $\Delta p_q(\nu)$ is the difference of the polarisabilities of the medium particles in the ground state and at the qth excited level at the frequency of the probe laser.

Under optical pumping of laser crystals (at frequencies in the visible and near-IR regions lying far from the resonance absorption frequencies of a matrix), the main contribution to the electronic RI changes is provided by changes in the population of metastable activator-ion levels. In this case, the dominant contribution to RI changes is due to the levels with the maximum population and highest polarisability. As is known, the polarisability of each level at the measurement frequency ν is determined by the probabilities of all transitions from this level induced by radiation at this frequency:

O.L. Antipov, O.N. Eremeikin, A.P. Savikin Institute of Applied Physics, Russian Academy of Sciences, ul. Ul'yanova 46, 603950 Nizhni Novgorod, Russia; e-mail: antipov@appl.sci-nnov.ru

Received 21 April 2003
Kvantovaya Elektronika **33** (10) 861 – 868 (2003)
Translated by A.S. Seferov

$$p_q(v) = \frac{e^2}{4\pi^2 m} \sum_i \frac{f_{qi}(v_{qi}^2 - v^2)}{(v_{qi}^2 - v^2)^2 + (v\Delta v_{qi})^2}$$

$$= \frac{\lambda n_0}{8\pi^2 F_L^2} \sum_i \frac{\sigma_{qi} v \Delta v_{qi}(v_{qi}^2 - v^2)}{(v_{qi}^2 - v^2)^2 + (v\Delta v_{qi})^2}, \quad (2)$$

where e and m are the electron charge and mass, and f_{qi}, σ_{qi}, v_{qi}, and Δv_{qi} are, respectively, the oscillator strength, effective cross section, frequency, and linewidth of the transition between the energy levels with indices q and i.

For equal oscillator strengths of all transitions, the main contribution to the polarisability of a level [the largest terms in (2)] is provided by the transitions with frequencies nearest to the probe-radiation frequency. However, in actual media, the oscillator strengths may differ by several orders of magnitude. For example, in laser crystals doped with rare-earth ions, the oscillator strengths of weakly allowed transitions inside one electron shell (the $4f$ working shell for Nd^{3+} ions) is 2–3 orders of magnitude lower than the oscillator strengths of strong intershell transitions ($4f - 5d$ for Nd^{3+}) [4, 5]. Therefore, strong intershell transitions in these crystals may substantially contribute to the sum (2) even at frequencies positioned far from the resonances of these transitions (the resonances of the $4f - 5d$ transitions of Nd-containing crystals lie in the UV). This contribution can compete with the contribution of quasi-resonance weakly allowed transitions, to which transitions within the $4f$ shell belong.

Recent studies have shown that, upon intense broadband flashlamp pumping, the electron component of the RI changes in laser crystals containing Nd^{3+} ions reaches a rather high value ($\sim 5 \times 10^{-7}$) [5, 6]. Under such pumping, the electron component of the RI changes may be determined by populating both the upper level of the $^4F_{3/2}$ lasing transition and the high-energy quasi-metastable levels ($^2F(2)_{5/2}$, $^4D_{3/2}$, and $^2P_{3/2}$) of the $4f$ shell of Nd^{3+} ions (Fig. 1). An especially large contribution to RI changes may be provided by high-energy levels localised near the $5d$ shell. The polarisability of these levels may be several orders of magnitude higher than the polarisability of the $^4I_{9/2}$ ground state. Therefore, even a small population at high levels can lead to noticeable RI changes in laser crystals. High-energy levels can be populated due to transitions from both the ground state and the $^4F_{3/2}$ metastable level of Nd^{3+} ions (absorption from an excited state) (Fig. 1).

Recent spectroscopic studies of the mechanisms of population of the $^2F(2)_{5/2}$ level in Nd : YAG crystals additionally confirm such a possibility. As was shown, under combined pumping by a 808-nm diode laser, which ensures the population of the $^4F_{3/2}$ level, and the fourth harmonic (266 nm) of an additional pulsed Nd : YAG laser, an enhanced luminescence intensity (by a factor of > 10 compared to the pumping only by the fourth harmonic) from the $^2F(2)_{5/2}$ level is observed [10, 11]. The efficient filling of the $^2F(2)_{5/2}$ level under combined pumping is explained by the $4f - 5d$ transition induced by the fourth-harmonic photons from the excited state (the $^4F_{3/2}$ metastable level) to $5d$-shell levels. The fast $5d - 4f$ radiationless relaxation that follows the absorption leads to the population of upper levels of the $4f$ shell, including the fairly long-lived $^2F(2)_{5/2}$ level with a lifetime of ~ 3 μs [12, 13].

The available data on the mechanism of population of the high-energy Nd^{3+} ion levels made it possible to study the contribution of these levels to RI changes in laser crystals upon their selective excitation. The selective population of the electronic levels of a Nd : YAG crystal was achieved in our experiments by using the diode and combined (diode-laser and laser) pumping.

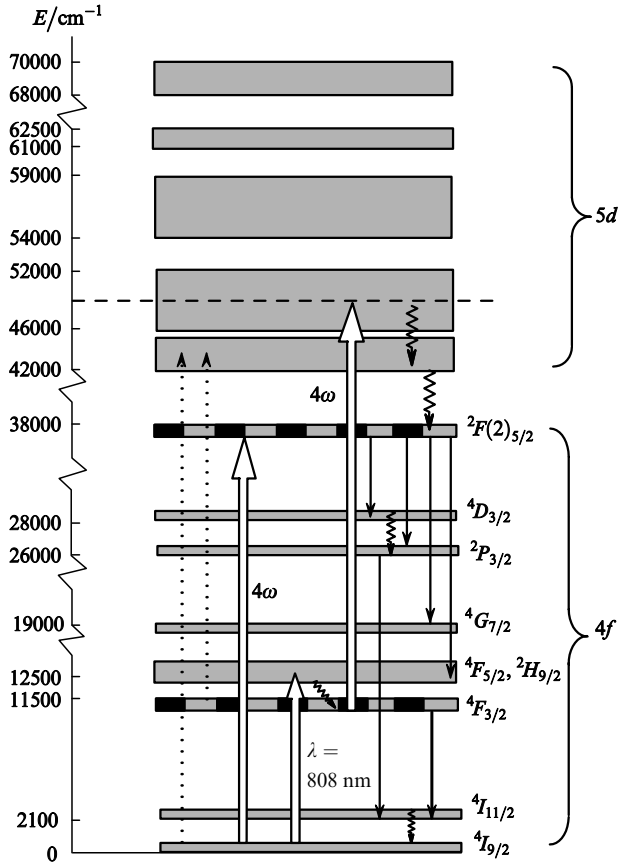

Figure 1. Energy level diagram of the of Nd^{3+} in a Nd : YAG crystal and its pumping by 808-nm diode-laser radiation and a beam of the fourth harmonic (4ω) at a wavelength of 266 nm.

3. Experimental setup

We studied the RI changes in a Nd : YAG crystal using a Jamin–Lebedev polarisation interferometer (Fig. 2) [14]. This laser crystal was grown by the Czochralski method (the atomic concentration of Nd^{3+} ions is 1 %) and cut as a cylinder 1 cm in length and 6 mm in diameter with a [001] orientation relative to the crystallographic axes. A cut parallel to its axis was made on the lateral cylindrical surface. The crystal was pumped through the area of this cut with dimensions of 3.5×10 mm (Fig. 3).

In the first run of experiments, the active Nd : YAG-crystal element (*4*) was pumped with a pulsed diode array (*3*) (produced by JENOPTIK) emitting a 808-nm light beam with a pulse power of < 300 W, a pulse duration of 200–300 μs, and a pulse repetition rate varied from several hertz to 1 kHz. In the second run of experiments, the Nd : YAG crystal (*4*) was pumped by the combined action of the diode array (*3*) and a beam of the fourth harmonic (266 nm, the photon energy is 37600 cm^{-1}) of a pulsed Nd:YAG laser (*2*). The laser-pulse duration, energy, and repetition rate were 10 ns, 2–4 mJ, and 10–12 Hz, respectively. A CDA crystal was used to double the Nd : YAG-

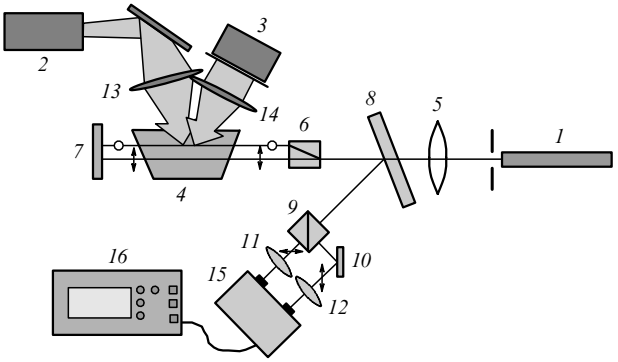

Figure 2. Schematic of the experimental setup: (*1*) He–Ne laser; (*2*) Nd : YAG laser ($\lambda = 266$ nm); (*3*) diode array ($\lambda = 808$ nm); (*4*) Nd : YAG crystal; (*5*, *11–14*) focusing lenses; (*6*) polarisation divider; (*7*, *10*) highly reflecting mirrors; (*8*) semitransparent mirror; (*9*) Glan prism; (*15*) two-channel differential amplifier; and (*16*) oscilloscope.

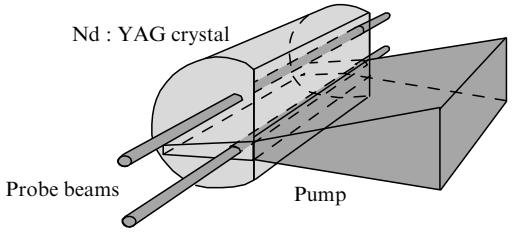

Figure 3. Schematic of pump and probe beams in a Nd:YAG crystal.

laser frequency, and the fourth harmonic was obtained by doubling the second harmonic in a DKDP crystal.

A linearly polarised beam from a probing He–Ne laser (*1*) passes through a focusing lens (*5*) with a 50-cm focal length and is split by a polarisation divider (*6*) into two parallel beams vertically spaced by 1.5 mm with mutually orthogonal polarisations and approximately equal intensities. After passing through the Nd : YAG crystal near the truncated lateral surface, the beams were reflected back from the totally reflecting mirror (*7*), transmitted through the crystal for the second time, and combined in the polarisation prism (*6*).

Focusing the pump beams at wavelengths of 808 and 266 nm inside the Nd : YAG crystal ensured the maximum overlap of the pumped region with one of the probe beams (Fig. 3). The pump-beam waist size was varied using focusing lenses (*13*) and (*14*) (Fig. 2).

RI changes in the pumped region of the Nd : YAG crystal, which changed the path difference between two probe beams, resulted in a change in the polarisation ellipticity of the combined output beam. To record the degree of ellipticity, the combined beam reflected by a semitransparent mirror (*8*) (Fig. 2) was again split by a Glan prism (*9*) into two beams with mutually orthogonal polarisations, and each of them was directed to its individual photodetector. To increase the sensitivity (to phase changes $\Delta\varphi \approx 10^{-3}$) and reduce the noise level by its compensation, we used a two-channel differential amplifier (*15*), to whose inputs photodetector signals were fed.

4. Changes in the refractive index of a diode-pumped Nd : YAG crystal

In the first run of experiments when the Nd : YAG crystal was pumped only by 808-nm radiation of the pulsed diode array, significant RI changes were observed. Interferometric-response oscillograms show an almost linear initial increase in the signal (during the pump-pulse duration of ~ 200 μs), and after the pump pulse terminates, the signal decays to zero with two well-resolved small (~ 250 μs) and large (5–10 ms) time constants (Fig. 4). The recorded signal is described by the sum of two exponents with a high accuracy (Fig. 5). The values of the signal-amplitude decrease on the fast and slow time scales were virtually identical for the system tuned to the maximum total signal. Equal amplitudes of the components in the signal approximation correspond to these values (Fig. 5). Note that the ratio of the amplitudes of these components was independent of the pump power.

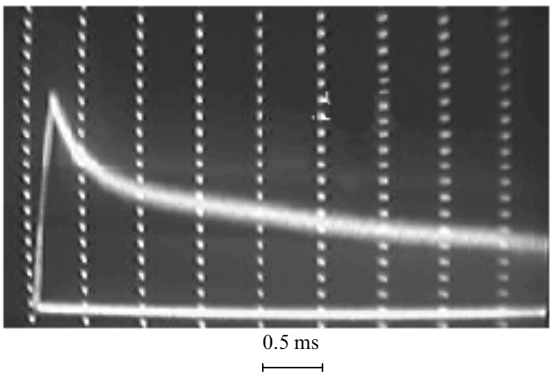

Figure 4. Oscillogram of an interferometric response of a Nd : YAG crystal pumped by 808-nm, 200-μs pulses from a diode array.

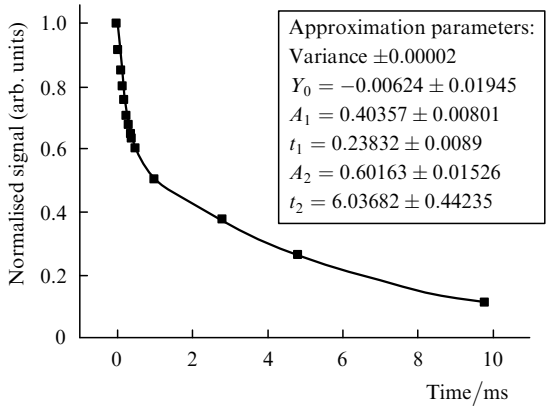

Figure 5. Approximation of an interferometric signal by a sum of two exponents using a formula $Y = Y_0 + A_1 \exp(-t/t_1) + A_2 \exp(-t/t_2)$ (a focusing lens with $F = 10$ cm).

When the pump beam was scanned inside the Nd : YAG crystal between the probe beams, the interferometric-signal amplitude at first decreased to zero (for the pump beam focused at the middle of the region between the probe beams) and then changed the sign and increased in magnitude to the initial value (when the region of passage of the second probe beam was pumped). The signal amplitude

reached the maximum when the pump beam overlapped one of the probe beams inside the crystal. Changes in the ratio between the amplitudes of the fast and slow signal components were observed during scanning. The fast component was more sensitive to the mutual position of the pump and probe beams and decreased almost immediately at a small shift of the pump beam from the probe-beam region, whereas the slow-component amplitude changed less significantly.

The revealed interferometric-signal dynamics indicates the existence of two mechanisms of RI changes of different natures, but both are associated with the pumping. The slow component of RI changes can be explained by the pump-induced heating and the heat relaxation on the crystal scale. The RI changes characterised by fast relaxation are explained by the excitation of the $^4F_{3/2}$ metastable level of the lasing transition, whose polarisability differs from the polarisability of the ground state. In fact, the fast-relaxation time (~ 250 μs), which is independent of the pump geometry, corresponds to the relaxation time of the $^4F_{3/2}$-level population, and the slow-relaxation time ($\sim 4-6$ ms), which depends on the size of the pumped region, corresponds to the temperature-equalisation time in the regions through which the probe beams are transmitted. Theoretical studies of the problem of heat conduction inside a Nd : YAG crystal have shown good correspondence of the temperature-relaxation dynamics in the probe-beam channels to the experimental behaviour of the slow component.

The values of RI changes depended on the pump-beam power density, which was varied by both increasing the radiation power and changing the size of the pumped region using lenses with different focal lengths (Figs 6, 7).

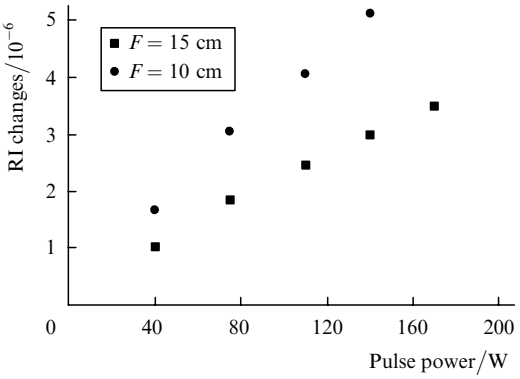

Figure 6. Maximum RI changes in a Nd : YAG crystal as a function of the pulse power of the diode array ($\lambda = 808$ nm) for lenses with different focal lengths F.

The experimentally obtained values of the electronic component of RI changes allow the pumped population of the $^4F_{3/2}$ level to be assessed by using the known difference of the polarisabilities of the $^4F_{3/2}$ metastable level and the $^4I_{9/2}$ ground state: $\Delta p(\nu) = 4 \times 10^{-26}$ cm^3 (for $\lambda > 630$ nm) [4, 5]. For a diode-pumped Nd : YAG crystal, the increase in the population of the $^4F_{3/2}$ (ΔN_F) metastable level can be estimated from formula (1) by assuming that only this level is populated and considering the crystal parameters $n_0 = 1.82$ and $F_L = 1.75$:

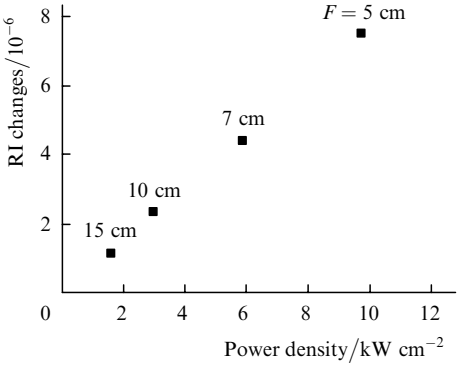

Figure 7. Maximum RI changes in a diode-pumped Nd : YAG crystal as a function of the power density ($\lambda = 808$ nm).

$$\Delta N_F \approx 2.4 \times 10^{24} \Delta n_e, \tag{3}$$

where ΔN_F is measured in terms of cm^{-3}. For the maximum measured RI changes $\Delta n_e \approx 5 \times 10^{-6}$, formula (3) yields $\Delta N_F \approx 10^{19}$ cm^{-3}, corresponding to the excitation of ~ 7 % of the total number of Nd^{3+} ions in the Nd : YAG crystal (since the 1% atomic concentration of Nd^{3+} ions corresponds to a bulk concentration of 1.38×10^{20} cm^{-3} [4, 7]).

The population of the upper level of the lasing transition in the diode-pumped Nd : YAG crystal can also be estimated by measuring the laser gain. The small-signal gain (at a resonance wavelength of 1.064) in the Nd : YAG crystal was measured in the diode-pumping geometry similar to the interferometric experiment. The gain of 50-μs pulses with an input intensity of < 1 W cm^{-2} was measured after two passes through the Nd : YAG amplifier (Fig. 8). These measurements allowed the population of the $^4F_{3/2}$ metastable level to be assessed using the formula for an unsaturated gain

$$\Delta N_F = \frac{\ln(P_{out}/P_{in})}{2\sigma l}, \tag{4}$$

where $\sigma = 3.5 \times 10^{-19}$ cm^2 is the amplification cross section of the Nd : YAG crystal at 1.064 μm, $l = 0.6$ cm is the length of the pumped region, and P_{out} and P_{in} are the laser-beam powers at the amplifier output (after two passes) and input, respectively. This estimate for ΔN_F agrees well with the data of interferometric measurements obtained at the

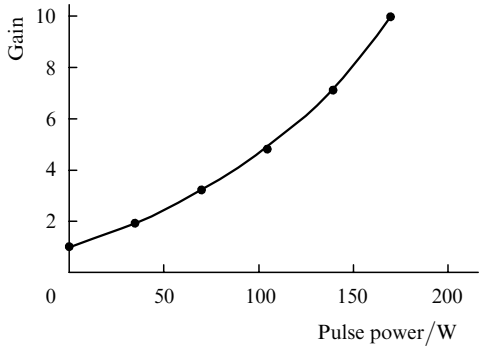

Figure 8. Small-signal gain (P_{out}/P_{in}) at $\lambda = 1064$ nm in a Nd:YAG crystal as a function of the diode-array pump pulse power.

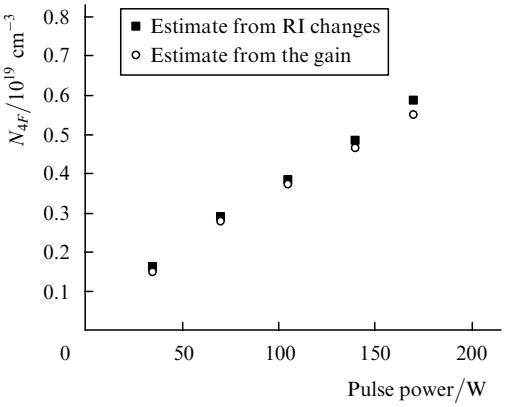

Figure 9. Estimate of the $^4F_{3/2}$-level population in a Nd : YAG crystal pumped by the diode array at 808 nm as a function of its pulse power.

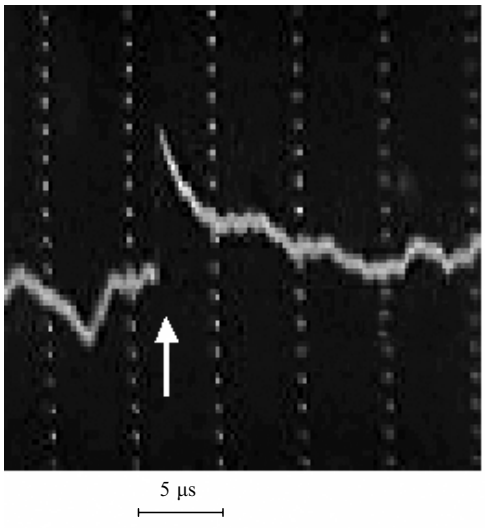

Figure 10. Oscillogram of an interferometric response of a Nd : YAG crystal simultaneously pumped by 808-nm radiation from a pulsed diode array and the fourth harmonic of a Nd : YAG laser (266 nm). The arrow indicates the position of a 10-ns pulse of the fourth harmonic.

same power of diode pump (Fig. 9). This conformity between different measurements testifies to a high accuracy in determining the electronic component of RI changes and correct estimates of the $^4F_{3/2}$-level polarisability.

5. Interferometric measurements upon combined pumping

At the beginning of the second run of our experiments, interferometric measurements were performed with a Nd : YAG crystal pumped only by pulses of the fourth harmonic (the pulse duration, energy, and wavelength were ~ 10 ns, < 2 mJ, and 266 nm). Slight RI changes ($< 2.5\times 10^{-7}$) with a slow relaxation observed after the termination of a pump pulse are consistently explained by thermal processes.

A significant increase in RI changes was recorded upon combined crystal pumping with pulses of the 808-nm diode-array radiation and 266-nm fourth harmonic. The pump beams were aligned inside the Nd : YAG crystal (Fig. 3). The time delay of the ~ 10-ns fourth-harmonic pulse relative to the diode-array pulse was varied between 200 and 250 μs. The maximum RI changes were observed when the fourth-harmonic pulse coincided with the trailing edge of the diode-array pulse.

Similarly to the experiment with the diode pumping, two components of RI changes with different decay dynamics were observed at the end of a fourth-harmonic pulse in the experiment with combined pumping: a rapidly decaying (~ 3 μs) and a slow 'thermal' component (with a millisecond time constant) (Fig. 10). The coincidence of the decay time of the fast component of RI changes with the decay time of the $^2F(2)_{5/2}$-level population (~ 3 μs [12, 13]) accounts for the presence of this component by the filling of this level.

Under combined pumping of the Nd : YAG crystal, the total RI changes were so large that, without taking special measures, the interferometer became saturated (the phase difference between its arms was $> \pi/2$). In this case, an intense heat release in the crystal influenced the shift of the interferometer's working point, thus complicating the precise determination of the RI changes at high pump energies. It was possible to measure the RI changes only at a decrease in the diode-array beam power and the fourth-harmonic pulse energy and also at a working-point shift. Estimating fast electronic changes in the RI at low pulse powers (20–30 W) of the diode array yielded $\Delta n_e \approx (1.2-1.5)\times 10^{-6}$ at a fourth-harmonic pulse energy of ~ 2 mJ (Fig. 11). In this case, the electronic components of RI changes turn out to be comparable to the total RI changes (they include the thermal component) recorded only under diode pumping of the same power.

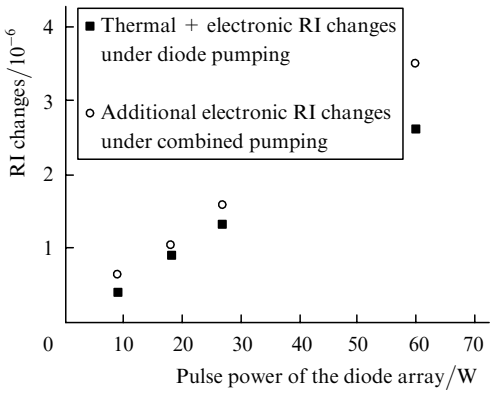

Figure 11. Maximum RI changes in a Nd : YAG crystal simultaneously pumped by the diode array ($\lambda = 808$ nm) and the fourth harmonic of a Nd : YAG laser (266 nm) as a function of the pulse power of the diode array (the fourth-harmonic pulse energy is 2.2 mJ).

As the fourth-harmonic pulse energy increased to 4–5 mJ, a virtually linear increase in the electronic RI changes was observed (the pulse power of the diode array was ~ 60 W) (Fig. 12). In this case, the electronic components of RI changes reached $\sim 6.0\times 10^{-6}$, whereas the total RI changes in the Nd:YAG crystal pumped only by the diode array were much lower ($\sim 2.5\times 10^{-6}$). A linear extrapolation of the electronic RI changes to high powers (up to 300 W) of diode-array pulses at a fixed energy (2.5 mJ) of the fourth harmonic yields $\sim 1.7\times 10^{-5}$, which

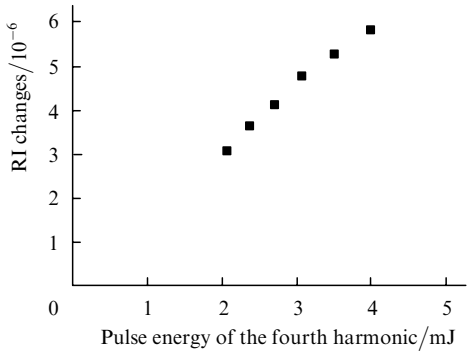

Figure 12. Electronic RI changes in a Nd : YAG crystal simultaneously pumped by the diode array ($\lambda = 808$ nm, the pulse power is 60 W) and the fourth harmonic of the Nd : YAG laser (266 nm) as a function of the fourth-harmonic energy.

is almost twice as large as the total RI changes under only the diode pumping.

The experimental data on the electronic RI changes under combined pumping make it possible to evaluate the polarisability of the $^2F(2)_{5/2}$ level. The difficulty of precisely determining the polarisability of this level is determined by the absence of direct measurements of its population. To indirectly assess the population of this level (N_{2F}), we should take into account that it is populated mainly due to transitions from the $^4F_{3/2}$ metastable level. This process can be described by the equation

$$\frac{\partial N_{2F}}{\partial t} + \frac{N_{2F}}{T_{2F}} = \beta_{df} \frac{\sigma_{\rm esa} I_{4\rm h} N_F}{h\nu_{4\rm h}}, \tag{5}$$

where $\sigma_{\rm esa}$ is the effective absorption cross section for quanta of the fourth harmonic from the $^4F_{3/2}$ level, T_{2F} is the $^2F(2)_{5/2}$-level relaxation time, $I_{4\rm h}$ is the pump intensity at a wavelength of 266 nm, $h\nu_{4\rm h}$ is the fourth-harmonic quantum energy, $\beta_{df} \leqslant 1$ is the dimensionless factor characterising the fraction of the absorbed energy spent for filling the $^2F(2)_{5/2}$ level (the difference of this factor from unity is determined by radiative transitions from the levels of the 5d shell and the $^2F(2)_{7/2}$ level, which lies between the $5d$ shell and the $^2F(2)_{5/2}$ level). In view of the fact that the pump pulse duration is $\tau_{4\rm h} \ll T_{2F} \ll T_{4F}$, from formula (5), we obtain

$$N_{2F} = \beta_{df} \frac{\sigma_{\rm esa} W_{4\rm h} N_F}{h\nu_{4\rm h} S_{4\rm h}}, \tag{6}$$

where $W_{4\rm h}$ is the fourth-harmonic pulse energy and $S_{4\rm h}$ is the cross-sectional area of the pump beam. Using the parameters of our experiment $W_{4\rm h} \approx 2$ mJ and $S_{4\rm h} \approx 0.02$ cm^{-2} and the reference data on the cross section of the absorption from the excited state ($\sigma_{\rm esa} \approx 7 \times 10^{-19}$ cm^2 [15, 16]), relation (6) yields

$$N_{2F} \approx 0.047 \beta_{df} N_F. \tag{7}$$

It follows from (7) that, in our experimental conditions, only a small fraction of Nd^{3+} ions moves from the $^4F_{3/2}$ to the $^2F(2)_{5/2}$ level ($N_{2F} \approx 0.015 N_F$ at $\beta_{df} = 0.3$). On the other hand, it should be taken into account that the electronic RI changes measured under combined pumping at a 2-mJ fourth-harmonic pulse energy were approximately equal to the total RI changes at the same intensity of only diode pumping. This means that the $^2F(2)_{5/2}$-level polarisability is two orders of magnitude higher than that of the $^4F_{3/2}$ level. Note that the mutual position of the $^2F(2)_{5/2}$ level and levels of the $5d$ shell, which form several wide bands (42000 – 45000, 46000 – 52000, and 54000 – 59000 cm^{-1}) [12], indicates an increase in the polarisability of this level at the operating wavelength (1064 nm) compared to 633 nm (the energy of 1064-nm quanta is closer to the $4f - 5d$ absorption peak from the $^2F(2)_{5/2}$ level than the energy of 633-nm quanta).

6. Electronic RI changes at a wavelength of 1064 nm

A 633-nm He–Ne laser was used as a source of the probe beam in our experiments. However, in practice, it is more important to know the electronic component of RI changes at the wavelengths of laser transitions, in particular, at the wavelength of the most frequently employed lasing transition (1064 nm). Unfortunately, it is difficult to directly measure the RI changes at this wavelength using the interferometer, because the probe beam is amplified in the diode-pumped Nd : YAG crystal. Therefore, analytic estimates of the levels' polarisabilities at this wavelength are of interest. Such an estimate can be performed by scaling the quantities measured at 633 nm to a wavelength of 1064 nm.

For a diode-pumped Nd : YAG crystal, the electronic component of RI changes is determined by the population of the $^4F_{3/2}$ level and related to the difference of its polarisability from the polarisability of the $^4I_{9/2}$ ground state. To scale the difference of the polarisabilities of the $^4F_{3/2}$ and $^4I_{9/2}$ levels to a wavelength of 1064 nm, the total sum that follows from definition (2) can be divided into two parts: the first and second parts are determined by close $4f - 4f$ resonances and strong $4f - 5d$ transitions:

$$\Delta p_{FI}(\nu) = \Delta p_{FI}^{4f-4f}(\nu) + \Delta p_{FI}^{4f-5d}(\nu). \tag{8}$$

The difference of the polarisabilities for the Δp_{FI}^{4f-4f} resonance transitions is determined by the luminescence and absorption lines from the $^4F_{3/2}$ level and also by the absorption lines from the $^4I_{9/2}$ level. Since the parameters of the transitions from these levels are known to a sufficient degree, the Δp_{FI}^{4f-4f} value can be found analytically.

Analytic calculations of the resonance polarisability were performed for the wavelength of the maximum Nd : YAG gain (1064.2 nm). The polarisability of the $^4F_{3/2}$ level was calculated from formula (2) taking into account the 15 strongest amplifying (luminescent) transitions and three absorbing transitions (absorption from an excited state) [4, 17, 18]. The parameters of these transitions used in calculations (the line centres, transition cross sections at the line centres, linewidths) are listed in Table 1. The necessity of taking into account a large number of lines is associated with the fact that their dispersion contributions to the total polarisability are comparable in magnitude but have different signs (even the transitions at 946- and 1318-nm wavelengths that are rather far from 1064.2 nm provide appreciable contributions).

Numerical calculations of the polarisability determined by the amplifying (luminescent) transitions from the $^4F_{3/2}$ level yielded $p_{4F}^{\rm lum}(1064.2\ {\rm nm}) \approx 6.3 \times 10^{-27}$ cm^3. When the

Table 1. Parameters of the transitions from the $^4F_{3/2}$ level used in calculations.

Transition	λ/nm	$\Delta\nu$/cm^{-1}	$\sigma/10^{-19}$ cm^2
$^4F_{3/2} \rightarrow {}^4I_{9/2}$	869.0	13*	0.41*, 0.41**
	875.4	10*	0.11*, 0.11**
	879.2*, 879.1**	18*	0.13*
	884.4	19*	0.42*
	885.8*, 885.7**	19*	0.35*
	891.1*, 891.0**	10*	0.24*
	893.4*, 893.2**	31*	0.05*
	900.0*, 899.9**	31*	0.12*
	938.6*, 938.5**	10*	0.48*, 0.35**
	956.1*, 946.0**	9*	0.51*, 0.77**
$^4F_{3/2} \rightarrow {}^4I_{11/2}$	1052.1	4.5*	0.95*, 1.15**
	1054.9	4.5*	0.06*
	1061.5	4.6*, 3.6**	2.50*, 2.69**
	1064.2*, 1064.15**	5.0*	3.00*, 3.03**
	1064.4	4.2*	1.45*, 1.09**
	1068.2	6.5*	0.60*, 0.77**
	1073.7	4.6*	1.65*, 1.49**
	1077.9	7.0*	0.77*, 0.68**
	1105.5	11.0*	0.16*, 0.13**
	1111.9	10.2*	0.36*, 0.43**
	1115.8	10.6*	0.42*, 0.40**
	1122.5	9.9*	0.40*, 0.46**
$^4F_{3/2} \rightarrow {}^4I_{13/2}$	1318.7, 1318.4**	4.0*	0.95*, 0.64**
	1320.3	4.6*	0.23*
	1333.5*, 1333.1**	3.0*	0.44*
	1335.1	3.3*	0.54*, 0.53**
	1338.1	4.0*	1.00*, 0.64**
	1341.9	6.0*	0.36*, 0.27**
	1353.3	4.0*	0.28*, 0.20**
	1357.2	4.0*	0.73*, 0.50**
	1415.0	8.5*	0.20*
	1427.1	7.0*	0.08*
	1432.0	10.0*	0.13*
	1444.4	9.0*	0.28*
$^4F_{3/2} \rightarrow {}^4G_{11/2}$	1040***	–	0.1***
$^4F_{3/2} \rightarrow {}^4G_{9/2}$	1067***	–	0.28***
	1074***	–	0.27***

*data on the luminescence lines [4]; **data on the luminescence lines [17]; ***data on the induced absorption [18].

absorption from an excited state was taken into account, this polarisability component decreased to p_{4F}^{4f-4f} (1064 nm) $\approx (1-4)\times 10^{-27}$ cm^3 (this large spread is due to a significant uncertainty in the linewidths of transitions for the absorption from an excited state [18]). An estimate of the polarisability of the $^4I_{9/2}$ level determined by the $4f-4f$ transitions with the absorption from the ground state yielded a negligibly small value at 1064.2 nm compared to p_{4F}^{4f-4f}. Therefore, it can be considered that the desired resonance polarisability component is determined only by the contribution of the $^4F_{3/2}$ level:

$$\Delta p_{FI}^{4f-4f}\,(1064.2\text{ nm}) \approx p_{4F}^{4f-4f}\,(1064.2\text{ nm}) \approx (1-4)\times 10^{-27}\text{ cm}^3. \quad (9)$$

The nonresonance polarisability component associated with the $4f-5d$ transitions at 1064.2 nm can be calculated on the basis of the Δp (633 nm) value, which was already known and also measured in our experiment. In fact, estimating the resonance polarisability component for the $^4I_{9/2}$ and $^4F_{3/2}$ levels at a probe-radiation wavelength of 633 nm (performed similarly to the estimate of this component at 1064.2 nm taking into account the absorbing $4f-4f$ transitions) yields values ~ 100 times lower than the experimentally determined electron component of the RI changes. Therefore, it can be considered that the difference of the $^4I_{9/2}$ and $^4F_{3/2}$-level polarisabilities (at $\lambda = 633$ nm) is determined only by the $4f-5d$ transitions:

$$\Delta p_{FI}\,(633\text{ nm}) \approx \Delta p_{FI}^{4f-5d}\,(633\text{ nm}) \approx 4\times 10^{-26}\text{ cm}^3. \quad (10)$$

The knowledge of Δp_{FI}^{4f-5d} (633 nm) allows us to evaluate Δp_{FI}^{4f-5d} (1064 nm). To do this, let us use the general expression (2), assuming that, for the $4f-5d$ transitions from the $^4F_{3/2}$ and $^4I_{9/2}$ levels, the oscillator strengths are identical [19]. For probe frequencies ν that lie far from the frequencies of the $4f-5d$ resonances ($(\nu_{F,I}^{4f-5d})^2 - \nu^2 \gg \nu\Delta\nu_{F,I}^{4f-5d}$), we then obtain an estimate

$$\Delta p_{FI}^{4f-5d}(\nu) \approx \frac{A}{\left(\nu_F^{4f-5d}\right)^2 - \nu^2} - \frac{A}{\left(\nu_I^{4f-5d}\right)^2 - \nu^2}, \quad (11)$$

where A is a proportionality factor and $\nu_{F,I}^{4f-5d}$ are the frequencies of the $4f-5d$ transitions from the $^4F_{3/2}$ and $^4I_{9/2}$ levels, respectively.

If the values of Δp_{FI}^{4f-5d} (633 nm) and $\nu_{F,I}^{4f-5d}$ are known, using (11), the following estimate can be obtained:

$$\Delta p_{FI}^{4f-5d}\,(1064.2\text{ nm}) \approx 3.15\times 10^{-26}\text{ cm}^3. \quad (12)$$

This value of the nonresonance component of the difference of polarisabilities (12) exceeds the quasi-resonance component by more than an order of magnitude. Thus, the contribution of the frequency-remote but strong $4f-5d$ transitions at the maximum gain ($\lambda = 1064.2$ nm) to the total polarisability of the $^4F_{3/2}$ level (and also to the difference of the $^4F_{3/2}$- and $^4I_{9/2}$-level polarisabilities) far exceeds the contribution of the quasi-resonance weak $4f-4f$ transitions (in addition, their contributions partially compensate for one another). Therefore, the total difference of the $^4F_{3/2}$- and $^4I_{9/2}$-level polarisabilities can be estimated as

$$\Delta p_{FI}\,(1064.2\text{ nm}) \approx (3.2-3.5)\times 10^{-26}\text{ cm}^3. \quad (13)$$

Note that the conclusion of the dominant contribution of the $4f-5d$ transitions to the total polarisability of the $^4F_{3/2}$ level is not valid for all wavelengths. At the edge of the amplification lines of the $4f-4f$ lasing transitions, there are frequencies at which the resonance polarisability component is rather large and exceeds the contribution of remote $4f-5d$ lines.

Since the total differences of the $^4F_{3/2}$- and $^4I_{9/2}$-level polarisabilities at 633 and 1064.2 nm differ insignificantly, it can be expected that the electronic components of the RI changes at these wavelengths will be equal. Based on equalities (10) and (13) and formula (1), the following estimate of the electronic component of RI changes can be given at a 7% occupancy of the $^4F_{3/2}$ level: $\Delta n_e\,(1064.2\text{ nm}) \approx (4.0-4.4)\times 10^{-6}$. This value shows that, under pulsed diode pumping, the electronic component of the RI changes at 1064.2 nm is close to the thermal one.

Upon combined pumping that ensures the filling of the $^2F(2)_{5/2}$ level, the electronic component of the RI changes at 1064.2 nm is expected to be larger than that at 633-nm wavelength, since the polarisability of the $^2F(2)_{5/2}$ level at 1064.2 nm exceeds that at 633 nm.

7. Conclusions

Significant RI changes associated with different polarisabilities of the ground state of Nd^{3+} ions (the $^4I_{9/2}$ level) and the upper level of the $^4F_{3/2}$ lasing transition appear in a Nd : YAG crystal under intense diode pumping (808 nm). For diode-laser pulse durations of 200 – 300 μs, electronic RI changes are comparable to thermal ones. For a Nd : YAG crystal simultaneously pumped by diode-laser and fourth-harmonic (266 nm) Nd : YAG-laser pulses, an additional increase in the electronic RI changes, which is determined by the filling of the $^2F(2)_{5/2}$ high-energy level, is observed. These changes are significant at a lasing-transition wavelength of 1064.2 nm and may appreciably affect the lens power and light-beam aberrations in Nd : YAG crystals. The electron component of RI changes are expected to be also rather large in other Nd^{3+}-containing laser crystals with oxide matrices (Nd : YVO_4, Nd : $YalO_3$, etc.).

Acknowledgements. This work was supported by the Russian Foundation for Basic Research (Grant Nos 01-02-17674, 02-02-81042 Bel.2002a, and 00-15-9675), the Program 'Quantum and Nonlinear Processes' of the RF Ministry of Industry and Science, the Science for Peace NATO Foundation (Grant SfP 974143), and the International Science and Technology Centre (Grant ISTC/EOARD 1913p).

References

1. Riedel E.P., Baldwin G.D. *J. Appl. Phys.*, **38**, 2720 (1967).
2. Bubnov M.M., Grudinin A.B., Dianov E.M., Prokhorov A.M. *Kvantovaya Elektron.*, **5**, 464 (1978) [*Sov. J. Quantum Electron.*, **8**, 275 (1978)].
3. Mezenov A.V., Some L.N., Stepanov A.I. *Termooptika tverdotel'nykh lazerov* (Thermooptics of Solid-State Lasers) (Leningrad: Mashinostroenie, 1986) p. 32.
4. Powell R.C. *Physics of Solid-State Laser Materials* (New York – Berlin – Heidelberg: Springer, 1998) p. 109.
5. Antipov O.L., Kuzhelev A.S., Luk'yanov A.Yu., Zinov'ev A.P. *Kvantovaya Elektron.*, **25**, 891 (1998) [*Quantum Electron.*, **28**, 867 (1998)].
6. Antipov O.L., Kuzhelev A.S., Chausov D.V., Zinov'ev A.P. *J. Opt. Soc. Am. B*, **16**, 1072 (1999).
7. Koechner W. *Solid-State Laser Engineering* (Berlin – Heidelberg: Springer, 1999) Vol. 1, p. 406.
8. Guy S., Bonner C.L., Shepherd D.P., Hanna D.C., et al. *IEEE J. Quantum Electron.*, **34**, 900 (1998).
9. Fluck R., Hermann M.R., Hackel L.A. *Appl. Phys. B*, **70**, 491 (2000).
10. Antipov O.L., Eremeykin O.N., Vorob'ev V.A., et al. *Tech. Digest XVII Intern. Conf. Nonlinear Optics «ICONO 2001»* (Minsk: Inst. Phys. NASB, 2001) p. 253.
11. Antipov O.L., Eremeykin O.N., Savikin A.P. *Kvantovaya Elektron.*, **32**, 793 (2002) [*Quantum Electron.*, **32**, 793 (2002)].
12. Kramer M.A., Boyd R.W. *Phys. Rev. B*, **23**, 986 (1981).
13. Basiev T.T., Dergachev A.Yu., Orlovskii Yu.V., Osiko V.V., Prokhorov A.M. *Trudy IOF RAN*, **46**, 3 (1994).
14. Francon M., Mallick S. *Polarization Interferometers: Application in Microscopy and Macroscopy* (New York: Academic Press, 1971).
15. Bagdasarov Kh.S., Volodin I.S., Kolomiitsev A.I., et al. *Kvantovaya Elektron.*, **9**, 1158 (1982) [*Sov. J. Quantum Electron.*, **12**, 731 (1982)].
16. Dubinskii A.M., Stolov A.L. *Fiz. Tverd. Tela,* **27**, 2174 (1985).
17. Kaminskii A.A. *Lazernye kristally* (Laser Crystals) (Moscow: Nauka, 1975) p.198.
18. Kück S., Fornasiero L., Mix E., Huber G. *Appl. Phys. B*, **67**, 151 (1998).
19. Axe J.D. *Phys. Rev.*, **136**, A42 (1964).